



Efficient removal of manganese ions from aqueous medium using a recyclable polymeric nanocomposite: A study of adsorption parameters and thermodynamics

Ibrahim Hotan Alsohaimi

*Chemistry Department, College of Science, Jouf University, Sakaka, Saudi Arabia, Tel. +966 504904183,
email: chem-ihg@hotmail.com, ehalshaimi@ju.edu.sa*

Received 10 April 2018; Accepted 17 September 2018

ABSTRACT

Herein, hybrid polymeric nano-composite (HPNC) was used for manganese metal ions (Mn^{2+}) removal from aqueous solution. Different parameters were used for adsorption tests. The equilibrium studies were confirmed using Freundlich and Langmuir isotherms and the adsorption capacity was calculated to be 162 mg/g for Mn^{2+} by fitting the equilibrium data to the Langmuir model. The kinetic parameters showed that Mn^{2+} ions adsorption on HPNC followed pseudo-second-order kinetic model. Furthermore, the negative values of ΔG and ΔH evidence that Mn^{2+} adsorption on HPNC is an exothermic and spontaneous process in nature. The desorption studies displayed the best recovery of Mn^{2+} ions in 0.1 M HCl indicating that they can be recycled in industrial processes. Regeneration studies showed 41.40% and 40.26% loss in Mn^{2+} adsorption and recovery after four consecutive cycles, respectively. These findings suggest that HPNC has the promising application as an effective and economically feasible adsorbent for Mn^{2+} removal.

Keywords: Adsorption; Hybrid polymeric nano-composite; Regeneration; Exothermic

1. Introduction

Heavy metals discharged into the environment from industrial activities such as plating plants, metal finishing, mining, alloy and welding manufacturing cause adverse effects on the environment and public health such as lung cancer, hemochromatosis, gastrointestinal catarrh, restlessness and skin dermatitis [1]. Manganese affects the nervous system functions when the body exposure to the low level and may cause an irreversible Parkinson-like symptoms known as manganism, characterized by feebleness, emotionless facial expression, apathy, muscle pain, anorexia, slow speech, decreased mental status, tremor and slow clumsy movement of the limbs [2–4]. The greatest concern with heavy metals is their acute and long-term toxicity. Heavy metals are being regulated increasingly with new regulations reducing metal effluent limits to parts per billion (ppb) [5]. They can easily pass up the food chain and water supply through a number of pathways and many of them are known to be carcinogenic or toxic. The removal

of heavy metals from contaminated wastewater streams is an important challenge to prevent one of the main causes of the contamination of water and soil [5–7].

Manganese as the divalent ion (Mn^{2+}) is usually present in natural water and it is widely used in various industrial fields such as battery manufacturing, ferroalloys, welding and electrical coils. It is considered as emerging contaminant because of their organoleptic properties [6]. The maximum acceptable level for Mn^{2+} as set by United States Environmental Protection Agency (USEPA) is 0.05 mg/L in drinking water [8], while World Health Organization (WHO) has set the maximum acceptable limits for Mn^{2+} are 0.1 and 0.05 mg/L in drinking and ground water, respectively [5,7].

Several approaches have been proposed to remove pollutants from waters using ion exchange resins [9], some of which includes chemical oxidation or reduction, electrochemical treatment, ion exchange, chemical precipitation, evaporation, adsorption, membrane filtration [10], biosorption [11] and chelating resins. Some of these techniques such as evaporation, ion exchange, reverse osmosis, membrane process and adsorption procedure have

*Corresponding author.

been developed for the elimination and retrieval of heavy metals from waters [12–14]. Among of all these techniques, adsorption is one of the most suitable water treatment method and has attracts an enormous amount of attention because of new material types available and can be applied for the removal process [15]. Selective adsorption utilizing polymeric materials has generated increasing excitement. Generally, polymeric adsorbents can efficiently trap many of the heavy metals from aqueous solutions [16–19]. The choice of these adsorbents for the removal process because of their surface area, easy recycling, and high reusability [20–23].

In recent years, many works have been done on the preparation and characterization of a different hybrid polymer adsorbents and its application for heavy metals removal from aqueous medium. A several novel methods were proposed to synthesize these adsorbents by some of research groups [23–27]. Pan et al. removed heavy metals from polluted waters effectively through modified a polymer-based hybrid sorbent (HFO-001) [28]. Ge et al. prepared a novel modified magnetic nanoparticles (MNPs) with copolymers for heavy metal ions removal (Cd^{2+} , Zn^{2+} , Pb^{2+} and Cu^{2+}) from aqueous solution [29]. Iesan et al. obtained polymer-based hybrid adsorbents by hydrated ferric oxide “in situ” encapsulated into the porous structure of polymeric exchanges and their effectiveness removal of arsenic has been investigated from aqueous solutions [30]. Liu et al. prepared a series of a hybrid zwitterionic polymer adsorbents via N-[3-(trimethoxysilyl)propyl] ethylene diamine (TMSPEDA) or phenylaminomethyl trimethoxysilane (PAMTMS) and pyromellitic acid dianhydride (PMDA) ring-opening polymerization and their applications for Cu^{2+} removal and the separation and recovery of heavy metal ions from wastewater [31,32].

Recently, several novel nanomaterial adsorbents have been designed and developed for the removal of heavy metals from wastewater with improving the efficiency and adsorption capacities. So, nanomaterials are used as the novel ones to purify wastewater containing heavy metal ions due to these materials have large surface and high porosity. These two properties can have a positive impact on their adsorption performance. In comparison to traditional materials, nanostructure adsorbents have exhibited much higher adsorption efficiency and faster rates in water treatment [33–35]. The nanomaterials successfully used as environmentally friendly adsorbents, efficient, and cost-effective for the removal of different toxic substrates from wastewater such as heavy metals.

To describe behavior of adsorption of manganese ions onto polymeric nanocomposite (HPNC), Langmuir and Freundlich isotherms are used [36,37]. Experimental data were fitted to adsorption isotherm models, and selected the best isotherm fitted model for characterize equilibrium adsorption. Langmuir and Freundlich-types adsorption adsorption are considered to be a monolayer and a multi-layer process respectively. Adsorption equilibrium data which express the relationship between mass of HPNC adsorbed and concentration of Mn^{2+} .

The objective of this work was to apply of the synthesized polymer based hybrid nano-composite (HPNC) [38] and its suitability for highly effective removal of manganese ions (Mn^{2+}) from polluted waters. The adsorption isotherms, kinetics and thermodynamics studies for Mn^{2+} ions

adsorption were carried out to elucidate the adsorption process. The reusable stability of resultant adsorbent was investigated by the recycling experiments.

2. Materials and methods

2.1. Chemicals and instruments

[3-(2-Aminoethylamino)propyl] trimethoxysilane (AEPTEOS, purity: $\geq 80\%$), pyromellitic acid dianhydride (PMDA, purity: $\geq 97\%$), tetraethyl orthosilicate (TEOS) and N,N-Dimethylformamide anhydrous (DMF) were purchased from Aldrich (Sigma-Aldrich) and used as received. Manganese nitrate ($\text{Mn}(\text{NO}_3)_2 \cdot 4\text{H}_2\text{O}$) was from BDH Chemical. The stock solutions of 1000 mg/L Mn^{2+} were prepared by dissolving the salt in water. Other chemicals were of analytical grade. The concentrations of manganese were measured using flame atomic absorption spectrometry (FAAS, PerkinElmer, PinAAcle 900T). For pH measurement, a single electrode pH meter (Orion 5 star, Thermo Scientific, USA) was used.

2.2. Preparation of adsorbent

According to the reference [38], the preparation of a hybrid adsorbent was obtained on the basis of ring-opening polymerization of PMDA with AEPTEOS in DMF solution. The process of ring-opening polymerization of PMDA and AEPTEOS was carried out by adding 2 ml of TEOS and 4 ml of 4 M HCl to the above-prepared hybrid monomer and the reaction mixture was kept at 110°C for 3 h. During this process, the production of the Si–O–Si bonds in the hybrid monomer occurs through sol–gel reaction between Si and O, and then the composition was precipitated as a polymer based hybrid nano-composite. Finally, to obtain the final hybrid adsorbent, the resulting solid was washed and dried at 70°C for 12 h. The synthesis of hybrid polymeric nano-composite (HPNC) and is shown in Fig. 1.

To evaluate the surface morphology and composition of the adsorbent, scanning electron microscopy (SEM; Japan) coupled with energy dispersive X-ray (EDX; USA) analyzer was conducted before and after manganese adsorption. Shape and mean size of HPNC was investigated by using transmission electron microscopy (TEM; Philips CM120). Fourier transform infrared (FT-IR; Nicolet 6700 FT-IR Thermo Scientific) analysis was performed in the range 4000–400 cm^{-1} region with 32 scans to record the spectra of HPNC before and after manganese ion adsorption.

2.3. Adsorption studies

Batch mode adsorption studies of Mn^{2+} ions from aqueous solution were performed as follows: 0.010 g HPNC introduced into a 100 mL Erlenmeyer flasks, and then 25 ml of Mn^{2+} solution at different concentrations (initial concentrations (C_0): 5–250 mg/L) were added into each flask. Then solutions were equilibrated in shaker at 100 rpm for 1440 min.

Solid/solution phases at equilibrium were filtered through filter paper and filtrate for the residual Mn^{2+} ions concentration was determined by FAAS.

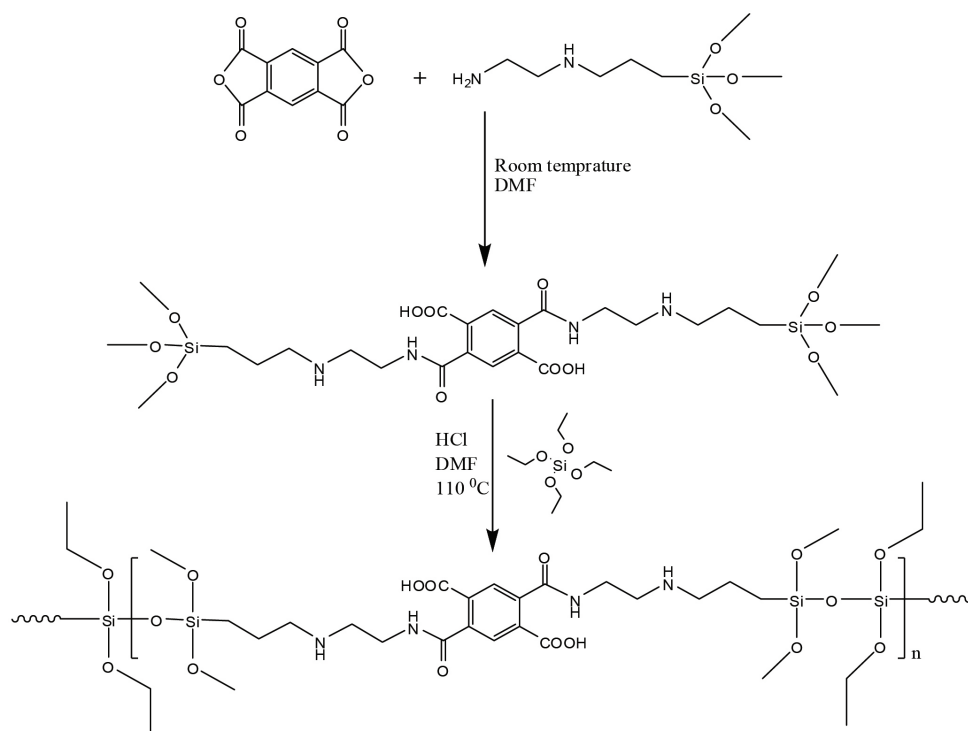


Fig. 1. The synthesis of hybrid polymeric nano-composite (HPNC).

The % adsorption of Mn^{2+} ions and adsorption capacity (q_e , mg/g) were calculated as:

$$\% \text{adsorption} = \frac{C_0 - C_e}{C_0} \times 100 \quad (1)$$

$$q_e = (C_0 - C_e) \times \frac{V}{m} \quad (2)$$

where C_e and C_0 (mg/L) are the equilibrium and initial concentrations of Mn^{2+} in aqueous solution, respectively, V is the volume of solution (L) and m is the mass of adsorbent (g).

The effect of pH was conducted in the range between 2.0–9.0 by adjusting the solution with 0.1 M NaOH and 0.1 M HCl. For the kinetic studies, the adsorption were conducted with the total volume 100 ml at varied Mn^{2+} ions initial concentration of the solutions (C_0 : 10, 50, and 100 $\text{mg}\cdot\text{L}^{-1}$) for a contact time in the range between 1–1440 min. Thermodynamic studies were also investigated for a temperature ranged 298–328 K. The dosage effect of a hybrid adsorbent on removing of Mn^{2+} has been studied with different dose of adsorbent (m : 0.01–0.05 g).

2.4. Desorption measurement

To evaluate the regeneration and reusability of the adsorbent, desorption and regeneration studies were carried out. For each cycle, 25 ml Mn^{2+} ions solution of initial concentration (C_0 : 25 $\text{mg}\cdot\text{L}^{-1}$) was adsorbed first by 0.010 g of adsorbent for 1440 min to reach adsorption equilibrium. To elute the adsorbed Mn^{2+} ions, the separated

adsorbent was treated with H_2SO_4 , HCl and HNO_3 (0.01 and 0.1 M) for 1440 min at 100 rpm and 298K. The calculation of %adsorption was determined as:

$$\% \text{desorption} = \frac{\text{Concentration of Manganese ions desorbed by eluent}}{\text{Initial concentration of Manganese ions adsorbed on adsorbent}} \times 100 \quad (3)$$

The adsorbent after desorption of Mn^{2+} ions was thoroughly washed with deionized water.

3. Results and discussion

3.1. Adsorbent characterization

The morphology of HPNC before and after adsorption was characterized using SEM. Fig. 2a presents the adsorbent particles agglomeration which led to a highly porous, irregular and rough surface morphology. However, the adsorption of Mn^{2+} ions on HPNC led to occupation of pores and the surface of HPNC is fully covered with Mn^{2+} ions (Fig. 2b). The elemental analysis by EDX confirmed adsorption of Mn^{2+} (Fig. 2b). The total pore volume and the Brunauer–Emmett–Teller (BET) surface area were 0.0553 cm^3/g and 40.78 m^2/g , respectively. Fig. 3a shows TEM image of HPNC. TEM image presented that the HPNC adsorbent was spherical, heterogeneous, aggregated surface and highly porous (Fig. 3a, inset). The average size of the HPNC at around 42 nm with size distribution which is also provided by the particle size distribution (Fig. 3b).

The FT-IR spectra of HPNC before and after manganese ions adsorption are presented in Fig. 4. A

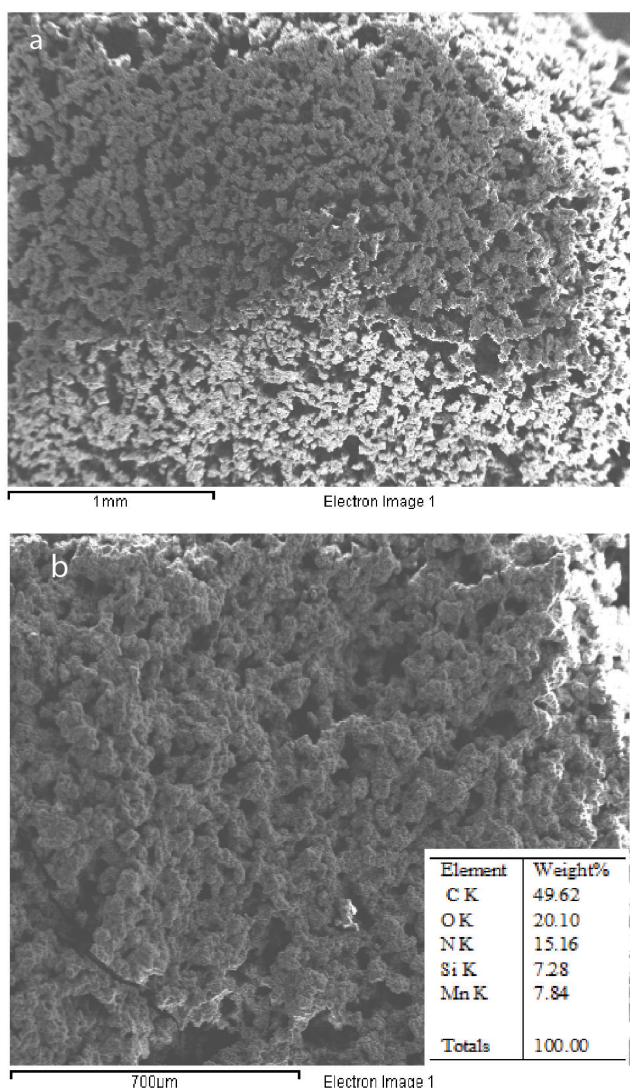


Fig. 2. SEM images before (a), and after Mn^{2+} (b) adsorption (insert EDX data) of HPNC.

broad band at 3200–3600 at 3563 cm^{-1} correspond to $-\text{OH}$ stretching vibration. The band at 2950 cm^{-1} corresponds to the $\text{C}-\text{H}$ stretching vibration. The adsorption band at 1776 cm^{-1} could be ascribed to stretching vibration of $\text{C}=\text{O}$ in acid anhydride due to the existence of PMDA in a hybrid polymer adsorbent [39]. A band at 1717 cm^{-1} was appeared due to the stretching frequencies of $-\text{C}=\text{O}$. A broad band is appeared at 1630 cm^{-1} due to $-\text{NH}$ stretching vibrations. Peak at 1400 cm^{-1} was related to the $\text{C}-\text{N}$ stretching vibration. The appearance of a broad band at $970-1180\text{ cm}^{-1}$ assigned to $\text{Si}-\text{O}-\text{Si}$ stretching was assigned due to the existence of branched or long siloxane chain. The main active sites for Mn^{2+} adsorption from aqueous phase were COOH and $\text{CO}-\text{NH}$ groups [40]. So, the FTIR spectrum of HPNC/Mn shows slight shifting and increasing in peak positions were observed after Mn^{2+} due to metal binding on the surface of the adsorbents. In details, slight peak shifting in position to 1613 cm^{-1} was observed after Mn^{2+} adsorption. The band at 1776 cm^{-1} was become more sharp support the coordination of the metal ions on to amide

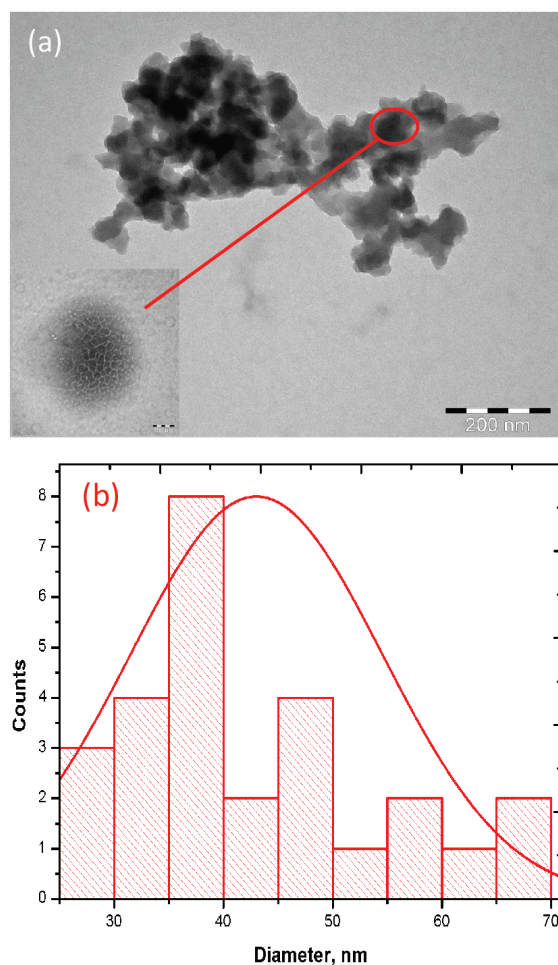


Fig. 3. (a) TEM image of HPNC (b) Particle size distribution for HPNC.

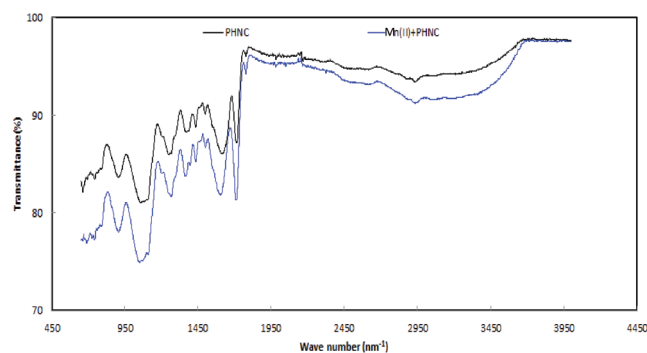


Fig. 4. FT-IR spectra before and after Mn^{2+} ions adsorption.

groups. Also, band at 1440 for $\text{C}-\text{N}$ slight shifting to 1390 indicating adsorption of Mn^{2+} onto $\text{C}-\text{N}$.

3.2. Effect of pH

The pH measurement of aqueous solution plays an important role to control the speciation and adsorption process of any adsorbate in the solution [41]. Fig. 5

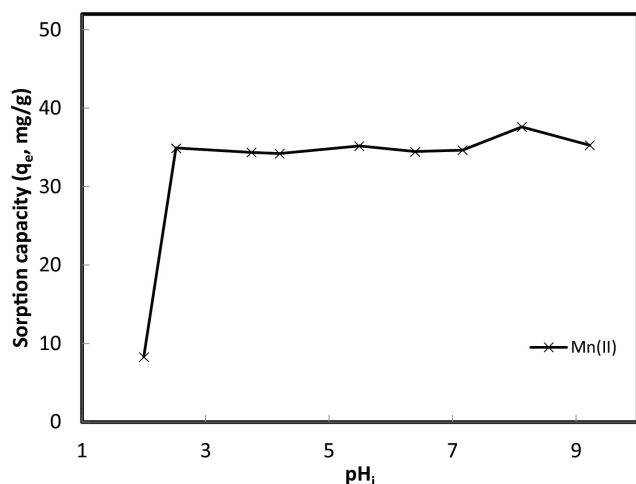


Fig. 5. Effect of pH on Mn²⁺ adsorption onto HPNC.

shows the effect of pH on the adsorption of Mn²⁺ ions from aqueous solution onto HPNC by keeping all other parameters constant (contact time 1440 min, HPNC dose 0.01 g, and temperature 25°C) in pH range 2–9. It was found that there is no adsorption preference to a specific pH and the adsorption capacity for Mn²⁺ metal ions was almost exactly the same except at pH 8, the adsorption capacity was reached up to 37.6 mg g⁻¹. After that, it started to slightly decrease in the adsorption capacity at pH 9. As expected, the adsorptive removal of Mn²⁺ ions was the same in the pH range 3–9; meaning that the adjusting step of pH of the solution for the adsorption of Mn²⁺ ions presented a negligible change in the adsorption capacity. So, the pH of the solution was then adjusted to pH 7 for further experiments.

3.3. Influence of initial concentration at various adsorbent dose and temperatures

The effects of initial Mn²⁺ ions concentrations ranged 5–250 mg/L at different temperatures (298–328 K) were studied. Generally, the adsorption capacity increased with increase in the initial Mn²⁺ ions concentration (Fig. 6). It can be seen also from the figure that the adsorption capacity decreases with the increase in temperature, indicating the adsorption of Mn²⁺ ions is of exothermic nature. The relation of the Mn²⁺ ions concentration to the adsorptive capacity of the adsorbent can be elucidated with the availability of active sites and the nature of the adsorbent. At 298 K, the adsorption capacity for higher initial concentration of Mn²⁺ ions shows highly effective up to 90 mg g⁻¹, whereas the maximum adsorption capacity for higher initial concentration of Mn²⁺ ions at 323 K was 75 mg g⁻¹. So, a higher initial concentration of Mn²⁺ ions tends to enhance the adsorption capacity.

The effect of HPNC dosage on the adsorption capacity of Mn²⁺ ions is shown in Fig. 7. It can be seen that adsorption of Mn²⁺ ions increases from 60 to 99.6%, as the dose of HPNC increased from 0.01 to 0.05 g. While the adsorption capacity for Mn²⁺ ions sharply decreased from 37.1 mg g⁻¹ to 13.8 mg g⁻¹. The decrease in the q_e of Mn²⁺ ions with increase in the adsorbent dose is might be due to the increase of free

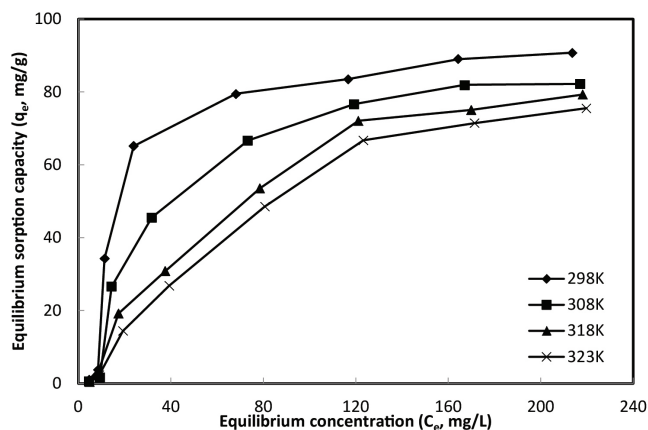


Fig. 6. Effect of concentration on Mn²⁺ adsorption onto HPNC at various temperatures.

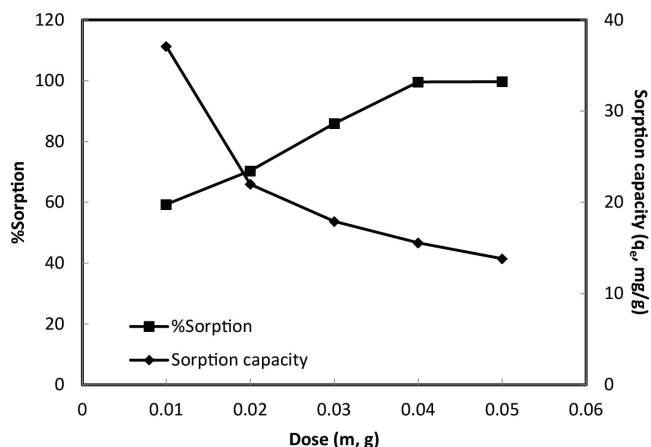


Fig. 7. Effect of HPNC dose on Mn²⁺ adsorption.

adsorption sites in the adsorption process. Moreover, an increase in adsorbent dosage might cause an overlapping or aggregation of adsorbent particles, leading to the total adsorption surface area decreasing available for Mn²⁺ ions to bind [42]. Thus, a dose of 0.01 mg/25 mL was selected as the optimum dose of HPNC for the further studies as it brought down the Mn²⁺ ions concentration to below the WHO acceptable limit.

3.4. Contact time effect on adsorption at various concentrations

The effect of contact time of Mn²⁺ adsorption at different concentrations were investigated on HPNC. It is observed that Mn²⁺ ions uptake was initially rapid, suggesting adsorption on HPNC surface and then diminished gradually until equilibrium is achieved. The adsorption equilibration time for Mn²⁺ ions at different concentrations varied between 460 and 700 min (Fig. 8). As we observed, the adsorption capacity increases with increase in Mn²⁺ ions concentration. At lower Mn²⁺ ions concentration, the adsorption was maximum for Mn²⁺ ions (11.4 mg/g) whereas at higher concentration, HPNC adsorption for the Mn²⁺ ions was more effective. The maximum adsorption

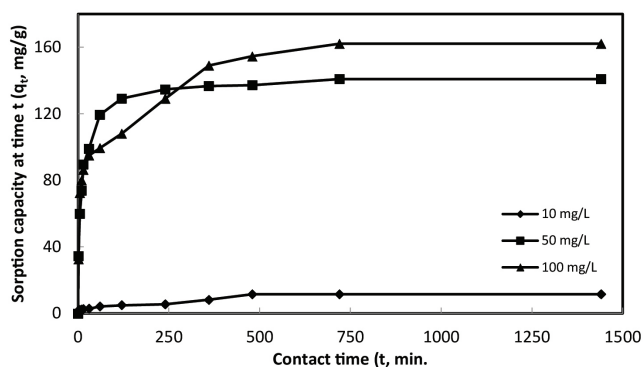


Fig. 8. Effect of contact time on Mn^{2+} adsorption onto HPNC at 298K.

capacity at equilibrium for Mn^{2+} ions at C_0 : 100 mg/L was 162 mg g^{-1} . The high removal efficiency of HPNC for Mn^{2+} ions may be attributed to the availability of abundant active sites of various CO–NH and –COOH groups on the HPNC [38].

3.5. Adsorption modeling

3.5.1. Adsorption isotherm

Adsorption isotherm studies is described the interaction between an adsorbate and adsorbent at equilibrium condition. Langmuir and Freundlich models were used to describe the adsorption of Mn^{2+} ions onto the HPNC. In linearized form Langmuir isotherm model can be expressed as [43]:

$$\frac{C_e}{q_e} = \frac{1}{bq_m} + \frac{C_e}{q_m} \quad (4)$$

The essential characteristic of Langmuir isotherm can be represent by separation factor (R_L), expressed as:

$$R_L = \frac{1}{1 + bC_0} \quad (5)$$

The value of R_L indicate the nature of adsorption process to be linear ($R_L = 1$), irreversible ($R_L = 0$), unfavorable ($R_L > 1$), favorable ($0 < R_L < 1$).

Freundlich isotherm model in linearized form can be represented as [44]:

$$\log q_e = \log K_f + \frac{1}{n} \times C_e \quad (6)$$

where q_e (mg/g), C_e (mg/L), q_m (mg/g), K_f (mg/g)(L/g) $^{1/n}$, and n are the adsorption capacity of adsorbent at equilibrium and the equilibrium concentration of the solute and the maximum monolayer adsorption capacity, the Langmuir and Freundlich adsorption constants, respectively.

Langmuir adsorption isotherm was derived to depict an independent monolayer adsorption of an adsorbate on a homogeneous and an adsorbent flat surface onto a surface with the number of active adsorption sites. The Freundlich isotherm was applied to explain the adsorption characteristics of an adsorbate onto the non-homogeneous surface of an adsorbent. The experimental data were fitted to the Langmuir isotherm as described by the higher correlation coefficient (R^2) values compared to Freundlich model (Table 1). These findings confirm the monolayer nature of the adsorption of Mn^{2+} ions onto HPNC. The values of R_L were < 1 which shows that the adsorptive process is favorable. (Table 2) shows comparison of the maximum adsorption capacities for Mn^{2+} ions of different adsorbents [45–51].

3.5.2. Adsorption kinetics

Kinetic study of adsorption is an important parameter to evaluate the adsorption process. The kinetic studies of Mn^{2+} metal ions adsorption at different initial concentrations using both pseudo-first-order [52] and pseudo-second-order [53] kinetic models were carried out:

$$\log(q_e - q_t) = \log q_e - \frac{K_1}{2.303} \times t \quad (7)$$

$$\frac{t}{q_t} = \frac{1}{K_2 q_e} + \frac{1}{q_e} \times t \quad (8)$$

where q_t , q_e , K_1 (1/min) and K_2 (g/mg-min) are the amount of Mn^{2+} ions adsorbed (mg/g) at time t and equilibrium, the pseudo-first-order and pseudo-second-order equilibrium rate constant, respectively.

Table 3 presents the parameters obtained from the kinetic models. The best fitted model to experimental data is compared by judging the correlation coefficients (R^2). The R^2 values of pseudo-second-order model for the adsorption of Mn^{2+} on HPNC were fitted well. A very good agreement is observed

Table 1
Adsorption isotherm parameters for Mn^{2+} adsorption on HPNC

Temperature (K)	$q_{m,exp}$ (mg/g)	Langmuir isotherm				Freundlich isotherm		
		$q_{m,cal}$ (mg/g)	b (L/mg)	R_L	R^2	K_f (mg/g) (L/mg) $^{1/n}$	n	R^2
298	90.75	98.04	0.0059	0.404	0.998	0.412	0.788	0.726
308	82.20	97.09	0.0283	0.124	0.998	0.135	0.759	0.889
318	79.30	113.64	0.0109	0.268	0.995	0.218	0.832	0.865
328	75.55	131.58	0.0065	0.381	0.994	0.139	0.785	0.905

Table 2
Comparison of the maximum adsorption capacities for Mn²⁺ ions of different adsorbents

Adsorbent	Experimental conditions	Equilibrium time (min)	q_m (mg/g)	Reference
Surfactant-modified alumina	C_o : 50 mg/L; T: 298K; m: 20 g/L pH: 6–7; T: 303K;	30	1.31	[42]
Lewatit TP 207	C_o : 20 mg/L; pH: 4; T: 298K; m: 0.05 g	120	140.85	[43]
Organophilic montmorillonite (OMMT) ceramics	C_o : 30–100 mg/L; pH: 6; T: 298K; m: 0.35 g	90	28.6	[44]
Calcium hydroxyapatite	C_o : 50 mg/L ; pH: 5.1; T: 300K; m: 1 g	30	58.99	[45]
Manganese oxide coated zeolite	C_o : 3.64 meq; pH: 6; T: 298K; m: 2.5 g L ⁻¹ ;	120	0.259 meq g ⁻¹	[46]
Clay mineral	C_o : 0.01 mol L ⁻¹ ; pH: 3.5; T: 298K; m: 0.05 g	48 h	74.6	[47]
Carbon aerogel	C_o : 1–5 mg/L; pH: 6; T: 318K, m: 10 g	48 h	1.275	[48]
Hybrid polymeric nano-composite (HPNC)	C_o : 5–250 mg/L ; pH: 7; T: 298 K, m: 0.010 g	460	162	This study

Table 3
Kinetic parameters for Mn²⁺ adsorption at varied concentration on HPNC

Initial Concentration (C_o , mg/L)	$q_{e,exp}$ (mg/g)	Pseudo-first-order kinetics			Pseudo-second-order kinetics		
		$q_{e,cal}$ (mg/g)	k_1 (1/min)	R^2	$q_{e,cal}$ (mg/g)	K_2 (g/mg-min)	R^2
10	11.45	9.36	0.0025	0.942	12.67	0.0110	0.987
50	140.93	55.19	0.0069	0.853	136.10	0.0001	0.987
100	162.15	93.71	0.0053	0.968	153.85	0.0003	0.988

between calculated equilibrium adsorption capacity values ($q_{e,cal}$) and the experimental ($q_{e,exp}$) for pseudo-second-order kinetic model values displaying better fitting of the model.

3.5.3. Thermodynamic studies

Thermodynamic considerations of Mn²⁺ ions adsorption was conducted at various temperatures (298, 308, 318, 328 K) through varying Mn²⁺ ions concentration of the solutions from 5 to 250 mg/L. Thermodynamic parameters such as enthalpy change (ΔH°), Gibb's free energy change (ΔG°), and entropy change (ΔS°) were calculated to tell the spontaneity of the adsorption reaction. Gibb's free energy change (ΔG°) is given as:

$$\Delta G^\circ = -RT \ln K_c \quad (9)$$

where $K_c = C_{Ae}/C_{e'} C_{Ae}$ and C_e (mg/L) are Mn²⁺ ions concentrations on HPNC and in the solution at equilibrium, respectively. K_c is an equilibrium constant.

The enthalpy (ΔH°) and entropy (ΔS°) changes were calculated from van't Hoff equation which is given as:

$$\ln K_c = \frac{\Delta S^\circ}{R} - \frac{\Delta H^\circ}{RT} \quad (10)$$

where R (8.314 J/mol-K) is a universal gas constant and T (K) is the absolute temperature.

Thermodynamic parameters for the adsorption of Mn²⁺ ions at various concentrations are presented in Table 4. The negative values of ΔG° and ΔS° presented the feasibility and spontaneity of Mn²⁺ ions adsorption onto the HPNC and a decrease in randomness at the solid/solution interface respectively. The adsorption of Mn²⁺ ions onto HPNC was physical and exothermic processes in nature due to the adsorptive forces weakening between Mn²⁺ ions and the active sites on the HPNC surface.

3.6. Desorption and regeneration studies

In order to evaluate the recovery of the adsorbed Mn²⁺ ions from HPNC, desorption and regeneration studies using various eluents were carried out. The optimum amount of Mn²⁺ ions was recovered with 0.1 M HCl (Fig. 9). Results showed that smallest ionic size of Cl⁻ compared to NO₃⁻ and SO₄⁻² might be attributed to more desorption of Mn²⁺ ions with 0.1 M HCl from adsorbent.

The economic feasibility of using HPNC adsorbent to remove Mn²⁺ ions from aqueous solution relied on its regeneration studies using 0.1 N HCl as an eluent. Regeneration studies showed that the adsorption of Mn²⁺ ions for four consecutive cycles varied between 90.32% and 40.40% on HPNC (Fig. 10). The recovery after four consecutive regeneration cycles of Mn²⁺ for HPNC reduced from 91.32% to 41.26%. The observed loss in Mn²⁺ ions recovery for HPNC after four consecutive cycles was 58.74%. As can be seen from Fig. 11, the structure of adsorbent hasn't been affected after 4th cycle adsorption/

Table 4
Thermodynamics parameters for the adsorption of Mn^{2+} on HPNC

C_o (mg/L)	$-\Delta H^\circ$ (kJ/mol)	$-\Delta S^\circ$ (J/ mol-K)	ΔG° (kJ/mol)			
			298 K	308 K	318 K	328 K
5	33.999	96.70	5.174	4.332	3.543	2.127
50	38.451	120.00	2.208	1.427	0.294	-0.841
250	15.516	33.40	5.411	5.099	4.834	4.392

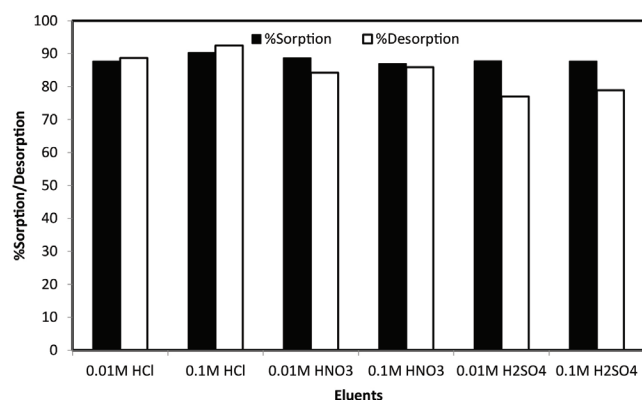


Fig. 9. Desorption efficiency plots of Mn^{2+} by various eluents.

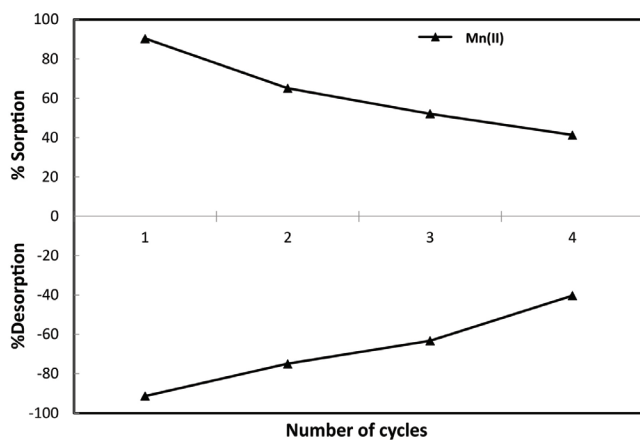


Fig. 10. Regeneration plot of HPNC for Mn^{2+} .

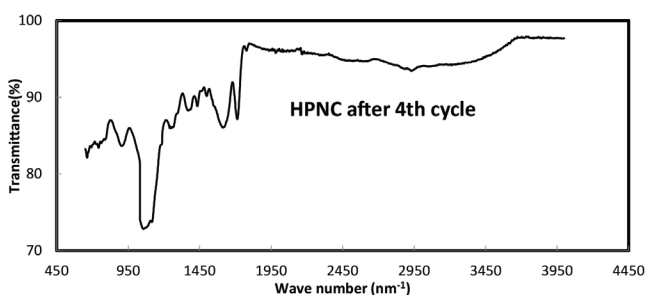


Fig. 11. FT-IR spectra after 4th cycle adsorption/desorption of Mn^{2+} ions.

desorption of Mn^{2+} ions confirming that the adsorption/desorption of Mn^{2+} ions does not destroy the active sites of the adsorbent.

4. Conclusions

The current work was accomplished to evaluate the adsorption efficacy of HPNC for Mn^{2+} ions removal through batch method. Solution pH presented a negligible change in the adsorption capacity and the uptake of Mn^{2+} ions was carried out at pH 7. The optimum adsorption capacity of HPNC for Mn^{2+} ions was found to be 162 mg/g. It was prominent that the % adsorption was decreased with increasing the temperature, which presented the exothermic nature of adsorption process. The adsorption followed the pseudo-second-order kinetic model, while adsorption isotherm well fitted to Langmuir model which confirmed monolayer adsorption. The changes in the FTIR peaks noticeably showed the adsorption of Mn^{2+} ions on HPNC. Desorption study revealed that the best recovery of Mn^{2+} ions from HPNC with 0.1 M HCl. The desorption mechanism was deduced as an ion-exchange process for replacing of Mn^{2+} ions with Cl^- of HCl.

Acknowledgment

The author thanks King Saud University for giving permission to conduct the analysis and for access to analytical equipment and Jouf University, too.

References

- [1] A. Aldawsari, M.A. Khan, B.H. Hameed, A.A. Alqadami, M.R. Siddiqui, Mercerized mesoporous date pit activated carbon: A novel adsorbent to sequester potentially toxic divalent heavy metals from water, *PIOS one*, 12 (2017) e0184493.
- [2] B. Michalke, S. Halbach, V. Nischwitz, Speciation and toxicological relevance of manganese in humans, *J. Env. Monit.*, 9 (2007) 650–656.
- [3] P. Roccaro, C. Barone, G. Mancini, F.G.A. Vagliasindi, Removal of manganese from water supplies intends for human consumption: a case study, *Desalination*, 210 (2007) 205–214.
- [4] B. Michalke, K. Fernsebner, New insights into manganese toxicity and speciation, *J Trace Elem Med Biol.*, 28 (2014) 106–116.
- [5] Guidelines for drinking-water quality, Recommendations, 4th ed., World Health Organization, Geneva 2011.
- [6] Z. Teng, J.Y. Huang, K. Fujita, S. Takizawa, Manganese removal by hollow fiber micro-filter. Membrane separation for drinking water, *Desalination*, 139 (2001) 411–418.
- [7] L. Ma, Y. Peng, B. Wu, D. Lei, H. Xu, Pleurotus ostreatus nanoparticles as a new nano-biosorbent for removal of $Mn(II)$ from aqueous solution, *Chem. Eng. J.*, 225 (2013) 59–67.
- [8] US EPA, Effluent guidelines program plan, 2008, <http://www.epa.gov/guide/304m/2008>.
- [9] T. Sata, Ion exchange membranes: preparation, characterization, modification and application, *R. Soc. Chem.*, (2004) 1–6.
- [10] G. Borbely, E. Nagy, Removal of zinc and nickel ions by complexation membrane filtration process from industrial wastewater, *Desalination*, 240 (2009) 218–226.
- [11] M.Y. Chang, R.S. Juang, Adsorption of tannic acid, humic acid, and dyes from water using the composite of chitosan and activated clay, *J Colloid Interface Sci.*, 278 (2004) 18–25.
- [12] R. Koivula, J. Lehto, L. Pajo, T. Gale, H. Leinonen, Purification of metal plating rinse waters with chelating ion exchangers, *Hydrometallurgy*, 56 (2000) 93–108.

- [13] S.H. Lin, S.L. Lai, H.G. Leu, Removal of heavy metals from aqueous solution by chelating resin in a multistage adsorption process, *J. Hazard. Mater.*, 76 (2000) 139–153.
- [14] K.A. Matis, N.K. Lazaridis, A.I. Zouboulis, G.P. Gallios, V. Mavrov, A hybrid flotation microfiltration process for metal ions recovery, *J. Membr. Sci.*, 247 (2005) 29–35.
- [15] I.H. Alsohaimi, M.A. Khan, Z.A. Alothman, M.R. Khan, M. Kumar, A.M. Almahri, Synthesis, Characterization, and Application of Fe-CNTs Nanocomposite for BrO_3^- Remediation from Water Samples, *J. Ind. Eng. Chem.*, 26 (2015) 218–225.
- [16] A. Denizli, G. Özkan, M.Y. Arica, Preparation and characterization of magnetic polymethylmethacrylate microbeads carrying ethylene diamine for removal of Cu(II), Pb(II), and Hg(II) from aqueous solutions, *J. Appl. Polym. Sci.*, 78 (2000) 81–89.
- [17] J.Y. Tseng, C.Y. Chang, Y.H. Chen, C.F. Chang, P.C. Chiang, Synthesis of micro-size magnetic polymer adsorbent and its application for the removal of Cu(II) ion, *Colloids Surf. A*, 295 (2007) 209–216.
- [18] S. Bassaid, M. Chaib, A. Bouguelia, M. Trari, Elaboration and characterization of poly (acrylic acid-co-crotonic acid) copolymers: application to extraction of metal cations Pb(II), Cd(II) and Hg(II) by complexation in aqueous media, *React. Funct. Polym.*, 68 (2008) 483–491.
- [19] O. Moradi, M. Aghaie, K. Zarea, M. Monajjemi, H. Aghaiea, The study of adsorption characteristics Cu²⁺ and Pb²⁺ ions onto PHEMA and P(MMA-HEMA) surfaces from aqueous single solution, *J. Hazard. Mater.*, 170 (2009) 673–679.
- [20] J.H. Qu, Research progress of novel adsorption processes in water purification: a review, *J. Environ. Sci.*, 20 (2008) 1–13.
- [21] V.K. Gupta, Suhas, Application of low-cost adsorbents for dye removal: a review, *J. Environ. Manage.*, 90 (2009) 2313–2342.
- [22] W.S. Wan Ngah, L.C. Teong, M.A.K.M. Hanafiah, Adsorption of dyes and heavy metal ions by Chitosan composites: a review, *Carbohydr. Polym.*, 83 (2011) 1446–1456.
- [23] B.J. Pan, B.C. Pan, W.M. Zhang, Development of polymeric and polymer-based hybrid adsorbents for pollutants removal, *Chem. Eng. J.*, 151 (2009) 19–29.
- [24] T.F. De Oliveira, E.S. Ribeiro, M.G. Segatelli, C.R.T. Tarley, Enhanced sorption of Mn²⁺ ions from aqueous medium by inserting protoporphyrin as a pendant group in poly(vinylpyridine) network, *Chem. Eng. J.*, 221 (2013) 275–282.
- [25] H.A. Panahi, M.S. Zadeh, S. Tavangari, E. Moniri, J. Ghassemi, Nickel adsorption from environmental samples by ion imprinted aniline-formaldehyde polymer, *Iran. J. Chem. Chem. Eng.*, 31 (2012) 35–44.
- [26] N.T. Tavengwa, E. Cukrowska, L. Chimuka, Modeling of adsorption isotherms and kinetics of uranium sorption by magnetic ion imprinted polymers, *Toxicol. Environ. Chem.*, 98 (2016) 1–12.
- [27] M. Saraji, H. Yousefi, Selective solid-phase extraction of Ni(II) by an ion-imprinted polymer from water samples, *J. Hazard. Mater.*, 167 (2009) 1152–1157.
- [28] B. Pan, H. Qiu, B. Pan, G. Nie, L. Xiao, L. Lv, W. Zhang, Q. Zhang, S. Zheng, Highly efficient removal of heavy metals by polymer-supported nanosized hydrated Fe(III) oxides: Behavior and XPS study, *Water research*, 44 (2010) 815–824.
- [29] F. Ge, M. Li, H. Ye, B. Zhao, Effective removal of heavy metal ions Cd²⁺, Zn²⁺, Pb²⁺, Cu²⁺ from aqueous solution by polymer-modified magnetic nanoparticles, *J. Hazard. Mater.*, 211–212 (2012) 366–372.
- [30] C. M. Iesan, C. Capat, F. Ruta, I. Udrea, Characterization of hybrid inorganic/organic polymer-type materials used for arsenic removal from drinking water, *React Funct Polym.*, 68 (2008) 1578–1586.
- [31] J.S. Liu, Y. Ma, T.W. Xu, G.Q. Shao, Preparation of zwitterionic hybrid polymer and its application for the removal of heavy metal ions from water, *J. Hazard. Mater.*, 178 (2010) 1021–1029.
- [32] Q. Dong, J. Liu, L. Song, G. Shao, Novel zwitterionic inorganic-organic hybrids: Synthesis of hybrid adsorbents and their applications for Cu²⁺ removal, *J. Hazard. Mater.*, 186 (2011) 1335–1342.
- [33] H. Sadegh, R.S. Ghoshekandi, A. Masjedi, Z. Mahmoodi, M. Kazemi, A review on Carbon nanotubes adsorbents for the removal of pollutants from aqueous solutions. *Int. J. Nano Dimens.* 7(2) (2016) 109
- [34] J. Theron, J. Walker, T. Cloete: Nanotechnology and water treatment: applications and emerging opportunities. *Crit. Rev. Microbiol.* 34(1) (2008) 43–69.
- [35] E.A. Dil, M. Ghaedi, A. Asfaram: The performance of nanorods material as adsorbent for removal of azo dyes and heavy metal ions: application of ultrasound wave, optimization and modeling. *Ultrason. Sonochem.* 34 (2017) 792–802.
- [36] J.C. Crittenden, K. Vaitheeswaran, D.W. Hand, E.W. Howe, E.M. Aieta, C.H. Tate, M.J. McGuire, M.K. Davis, *Water Res.*, 27 (1993) 715.
- [37] J.C. Crittenden, R.R. Trussell, D.W. Hand, K.J. Howe, G. Tchobanoglu, MWH's Water Treatment: Principles and Design, Wiley, (2012).
- [38] I.H. Alsohaimi, S.M. Wabaidur, M.Kumar, M.A. Khan, Z.A. Alothman, M.A. Abdalla, Synthesis, characterization of PMDA/TMSPEDA hybrid nano-composite and its applications as an adsorbent for the removal of bivalent heavy metals ions, *Chem. Eng. J.*, 270 (2015) 9–21.
- [39] J. Liu, Y. Ma, T.W. Xu, G.Q. Shao, Preparation of zwitterionic hybrid polymer and its application for the removal of heavy metal ions from water, *J. Hazard. Mater.*, 178 (2010) 1021–1029.
- [40] S. Prakash, M. Kumar, B.P. Tripathi, V.K. Shahi, Sol-gel derived poly(vinyl alcohol)-3-(2-aminoethylamino) propyltrimethoxysilane: Cross-linked organic-inorganic hybrid beads for the removal of Pb(II) from aqueous solution, *Chem. Eng. J.*, 162 (2010) 28–36.
- [41] Y. Ren, H.A. Abbood, F.B. He, H. Peng, K.X. Huang, Magnetic EDTA-modified Chitosan/SiO₂/Fe₃O₄ adsorbent: preparation, characterization, and application in heavy metal adsorption, *Chem. Eng. J.*, 226 (2013) 300–311.
- [42] A. Ozer, G. Akkaya, M. Turabik, Biosorption of Acid Red 274. (AR 274) on *Enteromorpha prolifera* in a batch system, *J. Hazard. Mater.*, B126 (2005) 119–127.
- [43] I. Langmuir, The adsorption of gases on plane surface of glass, mica and platinum, *J. Am. Chem. Soc.*, 40 (1916) 1361–1403.
- [44] H.M.F. Freundlich, Over the adsorption in solution, *J. Phys. Chem.*, 57 (1906) 385–470.
- [45] M.U. Khobragade, Anjali Pal. Fixed-bed column study on removal of Mn(II), Ni(II) and Cu(II) from aqueous solution by surfactant bilayer supported alumina. *Sep. Sci. Technol.*, 51 (2016) 1287–1298.
- [46] S. Bao, W. Hawker, J. Vaughan. scandium loading on chelating and solvent impregnated resin from sulfate solution. *Solvent Extr. Ion Exch.*, 36 (2018) 100–113.
- [47] A.A. Bakr, N.A. Sayed, T.M. Salama, I. Othman Ali, R.R. Abdel Gayed, N.A. Negm. Potential of Mg–Zn–Al layered double hydroxide (LDH)/montmorillonite nanocomposite in remediation of wastewater containing manganese ions. *Res. Chem. Intermed.*, 44(2018) 389–405.
- [48] V.E. Badillo-Almaraz, C. López-Reyes, J.M. Soriano-Rodríguez. Equilibrium studies and modeling on the removal of 56Mn(II) by alumina and kaolinite. *J. Radioanal. Nucl. Chem.*, 316 (2018) 571–578.
- [49] E. Erdema, N. Karapinarb, R. Donata, The removal of heavy metal cations by natural zeolites, *J. Colloid Interf. Sci.*, 280 (2004) 309–314.
- [50] M.G. da Fonseca, M.M. de Oliveira, L. N.H. Arakaki, Removal of cadmium, zinc, manganese and chromium cations from aqueous solution by a clay mineral. *J. Hazard. Mater.*, B137 (2006) 288–292.
- [51] A.K. Meena, G.K. Mishra, P.K. Rai, C. Rajagopal, P.N. Nagar, Removal of heavy metal ions from aqueous solutions using carbon aerogel as an adsorbent. *J. Hazard. Mater.*, B122 (2005) 161–170.
- [52] S. Lagergren, About the theory of so-called adsorption of soluble substances, *K. Sven. Vetenskapskad. Handl.*, 24 (1898) 1–39.
- [53] Y.S. Ho, G. McKay, The kinetics of sorption of divalent metal ions onto sphagnum moss peat, *Water Res.*, 34 (2000) 735–742.